Nuclear Materials and Energy 16 (2018) 221–225

Contents lists available at ScienceDirect

Nuclear Materials and Energy

journal homepage: www.elsevier.com/locate/nme

First-principles calculations of interaction between solutes and dislocations in tungsten

T. Tsuru[a,b,*], T. Suzudo[c]

[a] Nuclear Science and Engineering Center, Japan Atomic Energy Agency, 2-4 Shirakata, Tokai-mura, Ibaraki 319-1195, Japan
[b] Elements Strategy Initiative for Structural Materials (ESISM), Kyoto University, Yoshida, Honmachi, Sakyo-ku, Kyoto 606-8501, Japan
[c] Center for Computational Science and e-Systems, Japan Atomic Energy Agency, 2-4 Shirakata, Tokai-mura, Ibaraki 319-1195, Japan

ARTICLE INFO

Keywords:
Solution softening
Transmutation products
Dislocation
First-principles
Tungsten alloys

ABSTRACT

Changes in mechanical properties due to transmutation products (Re and Os) in W alloys is a central issue for plasma-facing materials in fusion reactors. We conducted density functional theory calculations to investigate the effect of Re, Os, and other 5d solutes on core structure and motion of screw dislocations associated with plastic deformation. Ir, Pt, Au, and Hg solutes show strong attractive interactions with screw dislocations, causing solution strengthening by the pinning mechanism. On the other hand, Hf, Ta, and Re cause softening by facilitating dislocation motion around solutes. This prediction corresponds well with the experimental observation of softening behavior in W-Re alloys.

1. Introduction

Tungsten (W) is a potential candidate for plasma-facing materials in fusion reactors due to its high melting point and thermal conductivity, as well as its high resistance to neutron sputtering [1–8]. Structural materials exposed to high deuterium and tritium fluxes under 14 MeV neutron irradiation, which releases significant amounts of transmutation products such as hydrogen and helium, experience degradation of their physical and mechanical properties [9–11]. The relationship between trapping of transmutation gas products and surface damage has been widely investigated [12–15]. The other important aspect of neutron irradiation in fusion reactors is the transmutation products of W [16]. Neutron irradiation produces increasing amounts of 5*d* metals such as rhenium (Re) and osmium (Os) with increasing fluxes, where Re is initially produced and then Os is created from Re. The stability of these transmutation products is a central issue when W alloys are used in fusion reactors, since fusion products may alter the mechanical properties of structural materials. The changes in mechanical properties, such as hardness and microstructure, due to irradiation have been examined for pure W, W-Re, W-Os, and W-Re-Os alloys [17], and clear differences were found between Re and Os in terms of the effect of irradiation hardening. Hardness decreases with Re content up to 10 mass% for low-dose neutron irradiation (below 1.54 dpa), while it increases linearly with the total concentration of Re and Os at higher doses [18], where precipitation nucleated by the irradiation contributes directly to the hardness. More recently, the local distribution of Re in W-Re and W-Re-Ta alloys under irradiation has been investigated using atom probe tomography, revealing that Re clustering tends to occur in these alloys [19]. On the other hand, it has long been known that Re solutes in W alloys cause solution softening [20–23], and that this softening behavior depends on both temperature and alloy composition. In particular, W-Re alloys exhibit a strong ductilization tendency at low temperatures (below 300 K) and low solution concentrations (about 10 at.%) [21], which is thought to be due to the effect of Re solutes on the double kink nucleation process [22]. The effects of individual transmutation solutes on mechanical properties, as well as the formation of radiation defects such as voids and radiation-induced precipitation (RIP), are therefore of great importance for W alloys under neutron irradiation.

We have so far carried out first-principles and kinetic Monte Carlo calculations to investigate the formation of radiation defects such as RIP in W alloys [24–26]. The formation and motion of W-Re and W-Os pairs in perfect crystals and some mixed dumbbell structures provide an insight into the effect of these elements on radiation defect formation. It is also important to understand solid solution strengthening and softening behavior in W, since W is intrinsically brittle. Regarding the effect of individual solutes on mechanical properties, the solution softening observed at low temperatures was found to be common to various body-centered cubic (BCC) metals [27]. Screw dislocation motion is a fundamental plastic deformation mechanism in BCC metals, and therefore

* Corresponding author at: Nuclear Science and Engineering Center, Japan Atomic Energy Agency, 2-4 Shirakata, Tokai-mura, Ibaraki 319-1195, Japan.
E-mail address: tsuru.tomohito@jaea.go.jp (T. Tsuru).

https://doi.org/10.1016/j.nme.2018.07.007
Received 14 November 2017; Received in revised form 3 July 2018; Accepted 15 July 2018
Available online 21 July 2018

the fundamental properties of dislocation motion associated with the core structure in W [28] and the effect of Re solutes on dislocation core structure [29–33] were investigated by density functional theory (DFT) calculations, where some sophisticated models were proposed. The stress-dependent interaction energy and migration process of Re in W alloys was investigated using DFT and kinetic Monte Carlo calculations [32], and softening effect was investigated by DFT and theoretical models in cooperation with the interaction between solute and a screw dislocation [33]. However, the energy barrier for dislocation motion should be considered as well as the interaction energy. In the present study, we construct a dipole configuration of screw dislocations in a periodic cell and investigate in detail the effects of Re and other 5*d* solutes on the interaction energy with a screw dislocation and the energy barrier for the dislocation motion through DFT calculations.

2. Analysis method

The introduction of dislocations into our periodic cell was accomplished by applying a continuum linear elastic theory solution for a periodic dislocation dipole array [34] in BCC W with lattice constant $a_0 = 3.1715$ Å. We can effectively solve for the distortion field in the periodic cell using a Fourier series, where the elastic energy can be expressed in Fourier space associated with elastic constants. The distortion field was then chosen to minimize the total elastic energy, subject to the topological constraints imposed by the dislocations. The displacement field can be obtained via line integrals. The displacement field of dislocation dipole in a 135-atom supercell was then obtained. In the present study, screw dislocation core with the Burgers vector $1/2 < 111 >$ was considered. The position of dislocation and solutes were shown in Fig. 1, where the core structure of the screw dislocation dipole was visualized using a differential displacement (DD) map [35]. The unit cell vector of the supercell for a dislocation quadrupolar is $x = 5a_0[11\bar{2}]$, $y = 2.5a_0[11\bar{2}] + 4.5a_0[\bar{1}10] + (a_0/4)[111]$, and $z = (a_0/2)[111]$. We used two- and six-layer supercell models along the z direction with a total of 270 and 810 atoms, respectively to confirm the convergence of the size along the direction, and two solutes were introduced near each side of the dipole's dislocation cores. The interaction energy between the 5*d* solutes and the screw dislocation dipole was then evaluated. First-principles electronic structure calculations were carried out within the DFT framework using the Vienna Ab-initio Simulation Package (VASP) [36,37], with the Perdew–Burke–Ernzerhof generalized gradient approximation exchange-correlation density functional [38]. The Brillouin-zone k-point samplings were chosen using the Monkhorst–Pack algorithm [39], where $1 \times 1 \times 9$ and $1 \times 1 \times 3$ k-point samples along x, y, and z directions were used for structural relaxation of two- and six-layer models, respectively. We used a plane-wave energy cutoff of 400 eV, with a first-order Methfessel–Paxton scheme employing a smearing parameter of 0.1 eV. We ensured that the total energy converged to within 10^{-6} eV for all calculations. The relaxed configurations were obtained by the conjugate gradient method, and the search was terminated when the force on all atoms had reduced to 0.02 eV/Å. The energy barrier and saddle point during dislocation motion for pure W were evaluated by the nudged elastic band (NEB) method with nine replica images [40].

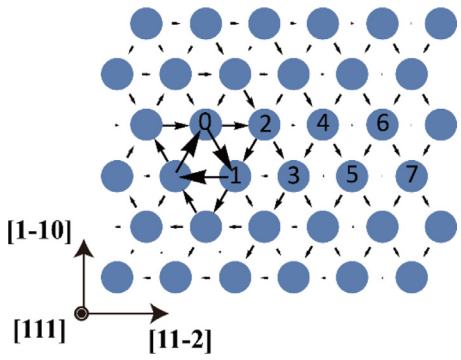

Fig. 1. The relative position of dislocation core and solutes, where the differential displacement vector is used to visualize the dislocation core.

3. Results and discussion

We first evaluated the interaction energy between the 5*d* solutes and the screw dislocation without atomic relaxation to understand the general features of the interaction, with the solutes being substituted at sites 0 to 7 according to Fig. 1. Fig. 2 shows the effect of the relative position (or distance) between the solutes and the dipole on the interaction energy for each solute, where the relative position of dislocation core is unchanged to constrain the dislocation motion influenced by high solute concentration. The interaction energy is defined as the energy difference between site 0 and furthest site from dislocation core. Strong attractive interactions were observed with the screw dislocation in iridium (Ir), platinum (Pt), gold (Au), and mercury (Hg), while hafnium (Hf), tantalum (Ta), and Re had relatively weak interactions and Os was in the middle. In addition, we found that the effective range of the interaction for most of the solutes was up to the 3rd nearest neighbor in the (111) plane, with little difference between the different solute types.

We then evaluated the actual interaction energy, considering atomic relaxation, for 1st nearest neighbor configuration (sites 0 and 1). Fig. 3(a) shows the interaction energies between all 5*d* solutes and a screw dislocation per a solute, where the solute is supposed to be substituted in every 2*b* units along the dislocation line. For confirmation of the convergence of the supercell size, we calculated the interaction energy only when each solute is substituted at site 0 using 6*b* unit supercell as shown in Table 1 and found that 2*b* unit reproduces the tendency well. The trends and absolute values are approximately the same as the ones calculated using unrelaxed configurations, indicating that the electronic interaction primarily determines the interaction energy. As discussed about d-band filling for bcc transition metals [41], the electronic interaction plays a significant role in the interaction energy in case of screw dislocation because there is no volumetric strain component unlike edge dislocations. Ir, Pt, Au, and Hg showed strong attractive interactions with the screw dislocation, resulting in solid solution hardening via the pinning mechanism. In addition, after atomic relaxation, the 3rd nearest neighbor configuration (site 3) for these solutes converged to the 1st nearest neighbor configuration (associated with site 1) due to the short-range strong attractive interaction with high solute concentration. On the other hand, since the interactions with Hf, Ta, and Re were not so strong, the dislocation did not move even when these solutes were substituted in 2nd nearest neighbor configuration. These results suggest that Hf, Ta, and Re at least do not induce solution strengthening.

Fig. 3(b) shows the relaxed core structures around typical Re, Os, and Au solutes, visualized by DD maps. We found that weakly-interacting solutes, such as Re, did not change the core structure, while those with attractive interactions, such as Au, causes reconstruction of the core structure, that is, the stable easy-core changes into a split core by the presence of these solutes. We should note, however, that this change of core structure is caused by high solute concentration and therefore, the interaction energy would be overestimated. There is still difficulty in simulating dilute alloys due to the computational cost though larger atomic models along dislocation line should be used.

The energy barrier to kink nucleation is important when discussing the effect of solutes on plastic deformation. The kink nucleation rate is expressed as the thermally activated process, which is associated with the external stress and the solute concentration as follows [42]:

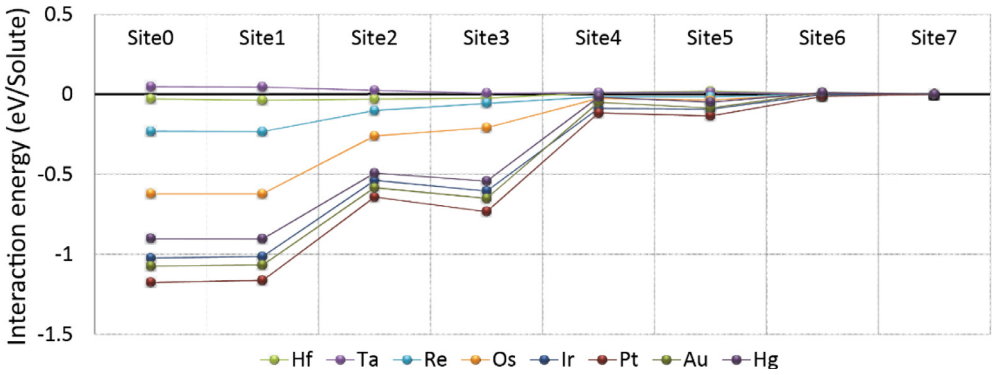

Fig. 2. Interaction energies per a solute with a screw dislocation dipole for 5*d* solutes at various lattice sites, where the energies are evaluated without atomic relaxation.

$$\nu_{dk}(\sigma, c) = (1-c)\nu_{dk}^{0}\exp\left(-\frac{\Delta H_{dk}(\sigma)}{k_B T}\right) + c\nu_{dk}^{0}\exp\left(-\frac{\Delta H_{dk}(\sigma) + E_{\mathrm{int}}(\sigma)}{k_B T}\right), \quad (1)$$

where c is the concentration, ν_{dk}^{0} is the attempt frequency of double kink nucleation, $\Delta H_{dk}(\sigma)$ is the activation enthalpy of pure W and $E_{\mathrm{int}}(\sigma)$ is the interaction energy under given stress σ. This relation indicates that the change in energy barrier of kink nucleation is directly affected by the interaction energy. As discussed above, however, the interaction energy is overestimated since the values are calculated by small atomic models with high solute concentration. In the present study, we estimated directly the Peierls barrier around the solutes as follows. First, we calculated the Peierls barrier in pure W using the NEB method associated with two adjacent easy-core configurations for the initial and final configurations. Here we obtained $E_{\mathrm{P}} = 0.18$ eV/2*b*, where 2*b* is the length of the dislocation line in the present study and corresponds to the unit cell size along the [111] direction. The saddle point configuration was then extracted for subsequent calculations. The solutes were then substituted at site 0 of this saddle point configuration, and atomic relaxation was carried out under the constraint that the displacement of the three atoms characterizing the dislocation core along [111] direction was fixed during relaxation to prevent the dislocation moving toward the easy-core configuration. As a result, the energy difference between the easy core and saddle point under the same constraint then provided an effective estimate of the effect of solutes on the Peierls barrier to dislocation motion without increasing the computational cost. The resulting energy differences and the relationships between the Peierls barrier and the interaction energy are shown in Figs. 4(a) and (b), respectively. The Peierls barrier per 2*b* unit is shown to indicate the solute concentration though only the effect per a solute should be discussed. The extremely strong correlation between

Table 1
Interaction energies between the solutes and the dislocation within the 1st nearest neighbor using 2*b* and 6*b* unit supercells.

	Hf	Ta	Re	Os	Ir	Pt	Au	Hg
E_{int} (2*b*)	–0.03	0.05	–0.23	–0.62	–1.14	–1.28	–1.17	–1.00
E_{int} (6*b*)	–0.09	0.03	–0.23	–0.63	–1.00	–1.18	–1.11	–0.98

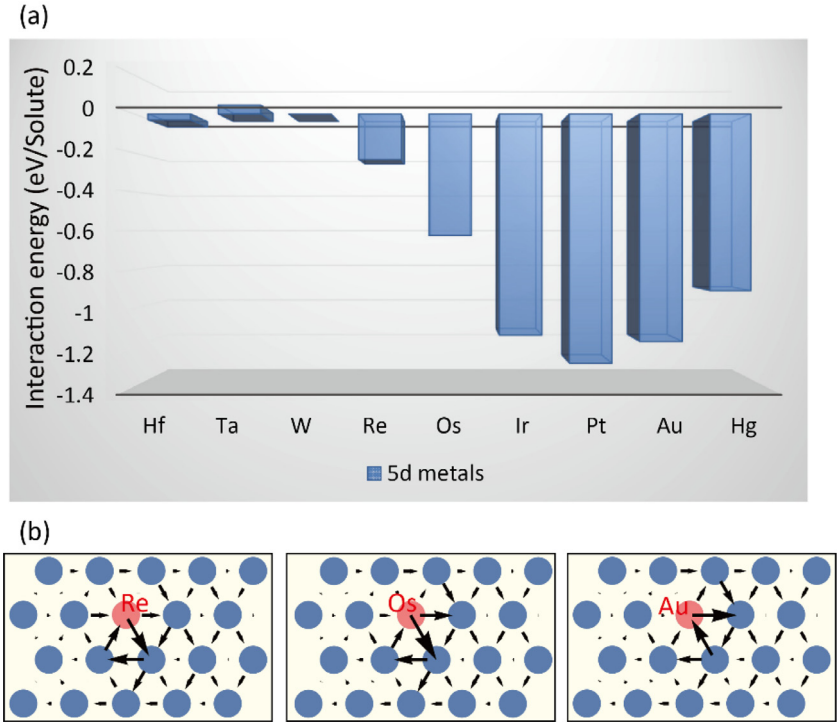

Fig. 3. Effects of different solutes on the dislocation core. (a) Interaction energies between the solutes and the dislocation for 1st nearest neighbor configuration after atomic relaxation. (b) DD maps for W-Re, W-Os, and W-Au.

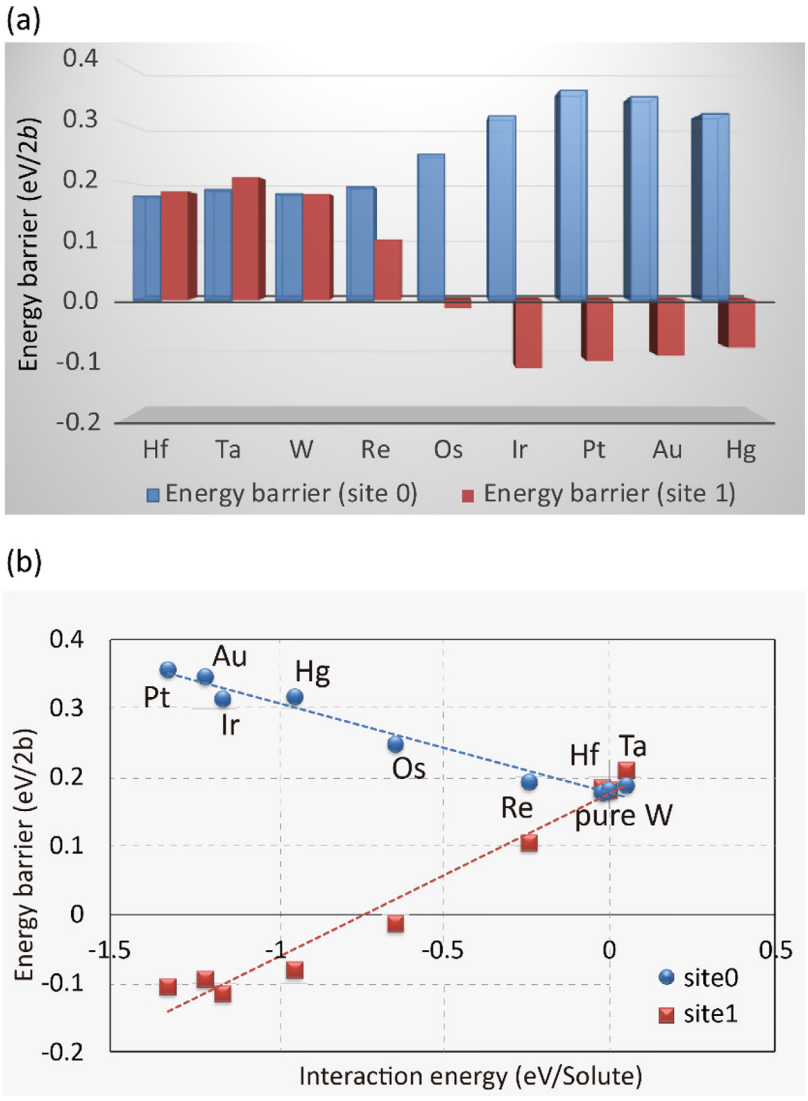

Fig. 4. (a) Energy barriers to dislocation motion for different solutes. (b) Relationship between the energy barrier and the interaction energy.

these energies indicates that the effect of solutes on dislocation motion is related to the interaction energy. In particular, with Ir, Pt, Au, and Hg solutes the Peierls barrier increases as the dislocation moves away from the solute, while the negative values indicate that there is no energy barrier when it is in 1st nearest neighbor configuration due to the attractive interaction. This negative barrier still arises from the high solute concentration, and both attractive and pinning forces are over estimated. Strong attractive interactions lead to solution strengthening due to the obstacle effect on kink migration as well as the pinning effect on athermal stress. In contrast, weakly-interacting Hf, Ta, and Re solutes reduce the Peierls barrier, and the barrier does not increase significantly as the dislocation moves away. Considering the weak attractive interactions between these solutes and the dislocation, these results suggest that Hf, Ta, and Re do not act as strong obstacles to kink migration, but they can attract screw dislocations moderately, increasing the primary nucleation rate. The predictions given above correspond reasonably well with the experimental results, where Re induces softening while Os and Ir increase hardness [17,18,21,22]. Our finding that softening is not only induced by Re but also by Hf. Accordingly, the solution softening behavior in W-Re and other W-based alloys is caused by reduction of the energy barrier to kink-nucleation due to the electronic interaction between the solutes and screw dislocations. More realistic calculations using thicker models are conducted to realize the individual effect of each solute in dilute alloys and the solid solution softening and hardening model using both interaction energy and energy barrier through DFT calculations for dilute alloy are being developed [43].

4. Conclusions

In this paper, we have investigated the effect of Re and other 5d solutes on solution softening/hardening in W via DFT calculations. Focusing on the motion and core structure of dislocations associated with plastic deformation, we constructed a quadrupolar model of a screw dislocation based on linear elasticity theory, and evaluated the interaction energies between solutes and a screw dislocation dipole. We found that Ir, Pt, Au, and Hg solutes showed strong attractive interactions, while Hf, Ta, and Re solutes showed relatively weak interactions. We have also proposed a method for approximately predicting the effect of solutes on the energy barrier to dislocation motion at low computational cost. The height of the energy barrier was found to be correlated with the interaction energy, indicating that Ir, Pt, Au, and Hg induce solution strengthening, while Hf, Ta, and Re cause softening by facilitating dislocation motion around solutes. These predictions, based on dislocation core calculations, correspond well with the experimental studies on mechanical behavior in W alloys.

Acknowledgments

This work was supported by JSPS Grant-in-Aid for Scientific Research (C) (No. 16K06714 and No. 15K06672). The authors acknowledge Prof. A. Hasegawa for helpful discussions. All simulations were performed on the large-scale parallel computer system with SGI ICE X at JAEA.

References

[1] G. Janeschitz, Plasma–wall interaction issues in ITER, J. Nucl. Mater. 290–293 (2001) 1–11.
[2] D. Naujoks, et al., Tungsten as target material in fusion devices, Nucl. Fusion 36 (1996) 671–587.
[3] Y. Ueda, K. Tobita, Y. Katoh, PSI issues at plasma facing surfaces of blankets in fusion reactors, J. Nucl. Mater. 313-316 (2003) 32–41.
[4] H. Bolt, V. Barabash, W. Krauss, J. Linke, R. Neu, S. Suzuki, N. YoshidaASDEX Upgrade Team, Materials for the plasma-facing components of fusion reactors, J. Nucl. Mater. 329–333 (2004) 66–73.
[5] R. Neu, Final steps to an all tungsten divertor tokamak, J. Nucl. Mater. 363–365 (2007) 52–59.
[6] A.R. Raffray, et al., High heat flux components-Readiness to proceed from near term fusion systems to power plants, Fusion Eng. Des. 85 (2010) 93–108.
[7] Y. Ueda, J.W. Coenen, Research status and issues of tungsten plasma facing materials for ITER and beyond, Fusion Eng. Des. 89 (2014) 901–906.
[8] A. Hasegawa, M. Fukuda, K. Yabuuchi, S. Nogami, Neutron irradiation effects on the microstructural development of tungsten and tungsten alloys, J. Nucl. Mater. 471 (2016) 175–183.
[9] B.I. Khripunov, et al., 18th Conference on Plasma-Surface Interactions, PSI 2015, 5-6 February 2015, Moscow, Russian Federation and the 1st Conference on Plasma and Laser Research and Technologies, 2015, pp. 63–67 PLRT 2015, 18-20 February 2015, Phys. Procedia 71.
[10] Y. Hatano, et al., Trapping of hydrogen isotopes in radiation defects formed in tungsten by neutron and ion irradiations, J. Nucl. Mater. 438 (2013) S114–S119.
[11] W.R. Wampler, R.P. Doerner, The influence of displacement damage on deuterium retention in tungsten exposed to plasma, Nucl. Fusion 49 (2009) 115023.
[12] N. Yoshida, H. Iwakiri, K. Tokunaga, T. Baba, Impact of low energy helium irradiation on plasma facing metals, J. Nucl. Mater. 337–339 (2005) 946–950.
[13] M. Zibrov, M. Baladen, T.W. Morgan, M. Mayer, Deuterium trapping and surface modification of polycrystalline tungsten exposed to a high-flux plasma at high fluences, Nucl. Fusion 57 (2017) 046004.
[14] M.J. Baldwin, R.P. Doerner, Helium induced nanoscopic morphology on tungsten under fusion relevant plasma conditions, Nucl. Fusion 48 (2008) 035001.
[15] A. Hasegawa, M. Fukuda, T. Tanno, S. Nogami, Neutron irradiation behavior of Tungsten, Mater. Trans. 54 (2013) 466–471.
[16] R.A. Causey, The use of tungsten in fusion reactors: a review of the hydrogen retention and migration properties, Phys. Scripta T94 (2001) 9–15.
[17] J.C. He, A. Hasegawa, M. Fujiwara, M. Satou, T. Shishido, K. Abe, Fabrication and characterization of W-Re-Os alloys for studying transmutation effects of W in fusion reactors, Mater. Trans. 45 (2004) 2657–2660.
[18] T. Tanno, A. Hasegawa, J. He, M. Fujikawa, S. Nogami, M. Satou, T. Shishido, K. Abe, Effects of transmutation elements on neutron irradiation hardening of tungsten, Mater. Trans. 48 (2007) 2399–2402.
[19] A. Xu, D.E.J. Armstrong, C. Beck, M.P. Moody, G.D.W. Smith, P.A.J. Bagot, S.G. Roberts, Ion-irradiation induced clustering in W-Re-Ta, W-Re and W-Ta alloys: an atom probe tomography and nanoindentation study, Acta Mater. 124 (2017) 71–78.
[20] G.A. Geach, J.R. Hughes, The alloys of rhenium and molybdenum or with tungsten and having good hightemperature properties, in: F. Benesovsky (Ed.), Plansee Proceedings, Pergamon Press, London, 1955, pp. 245–253.
[21] J.R. Stephens, W.R. Witzke, Alloy softening in group via metals alloyed with rhenium, J. Less Common Met. 23 (1971) 325–342.
[22] A. Luo, D.L. Jacobson, K.S. Shin, Solution softening mechanism of iridium and rhenium in tungsten at room temperature, Int. J. Refract. Met. Hard Mater. 10 (1991) 107–114.
[23] P.L. Raffo, Yielding and fracture in Tungsten and Tungsten-Rhenium alloys, J. Less-Common Met. 17 (1969) 133–143.
[24] T. Suzudo, M. Yamaguchi, A. Hasegawa, Stability and mobility of rhenium and osmium in tungsten: first principles study, Model. Simul. Mater. Sci. Eng. 22 (2014) 075006.
[25] T. Suzudo, M. Yamaguchi, A. Hasegawa, Migration of rhenium and osmium interstitials in tungsten, J. Nucl. Mater. 467 (2015) 418–423.
[26] T. Suzudo, A. Hasegawa, Suppression of radiation-induced point defects by rhenium and osmium interstitials in tungsten, Sci. Rep. 6 (2016) 36738.
[27] E. Pink, R.J. Arsenault, Low-temperature softening in body-centered cubic alloys, Prog. Mater. Sci. 24 (1979) 1–52.
[28] L. Dezerald, D. Rodney, E. Clouet, L. Ventelon, F. Willaime, Plastic anisotropy and dislocation trajectory in BCC metals, Nature Comm. 7 (2017) 11695.
[29] L. Romaner, C. Ambrosch-Draxl, R. Pippan, Effect of rhenium on the dislocation core structure in Tungsten, Phys. Rev. Lett. 104 (2010) 195503.
[30] H. Li, S. Wurster, C. Motz, L. Romaner, C. Ambrosch-Draxl, R. Pippan, Dislocation-core symmetry and slip planes in tungsten alloys: ab initio calculations and microcantilever bending experiments, Acta Mater. 60 (2012) 748–758.
[31] G.D. Samolyuk, Y.N. Osetsky, R.E. Stoller, The influence of transition metal solutes on the dislocation core structure and values of the Peierls stress and barrier in tungsten, J. Phys.: Condens. Matter 25 (2013) 025403.
[32] M.Z. Hossain, J. Marian, Stress-dependent solute energetics in W–Re alloys from first-principles calculations, Acta Mater. 80 (2014) 107–117.
[33] Y.-J. Hu, M.R. Fellinger, B.G. Bulter, Y. Wang, K.A. Darling, L.J. Kecskes, D.R. Trinkle, Z.-K. Liu, Solute-induced solid-solution softening and hardening in bcc tungsten, Acta Mater. 141 (2017) 304–316.
[34] M.S. Daw, Elasticity effects in electronic structure calculations with periodic boundary conditions, Comp. Mater. Sci. 38 (2006) 293–297.
[35] V. Vitek, R.C. Perrin, D.K. Bowen, The core structure of ½(111) screw dislocations in b.c.c. crystals, Philos. Mag. 21 (1970) 1049–1073.
[36] G. Kresse, J. Hafner, Ab initio molecular dynamics for liquid metals, Phys. Rev. B47 (1993) 558–561.
[37] G. Kresse, J. Furthmuller, Efficient iterative schemes for ab initio total-energy calculations using a plane-wave basis set, Phys. Rev. B54 (1996) 11169–11186.
[38] J.P. Perdew, K. Burke, M. Ernzerhof, Generalized gradient approximation made simple, Phys. Rev. Lett. 77 (1996) 3865–3868.
[39] H.J. Monkhorst, J.D. Pack, Special points for Brillouin-zone integrations, Phys. Rev. B13 (1976) 5188–5192.
[40] G. Henkelman, B.P. Uberuaga, H. Jónsson, A climbing image nudged elastic band method for finding saddle points and minimum energy paths, J. Chem. Phys. 113 (2000) 9901–9904.
[41] H. Li, C. Draxl, S. Wurster, R. Pippan, L. Romaner, Impact of d-band filling on the dislocation properties of bcc transition metals: The case of tantalum-tungsten alloys investigated by density-functional theory, Phys. Rev. B 95 (2017) 094114.
[42] D.R. Trinkle, C. Woodward, The chemistry of deformation: how solutes soften pure metals, Science 310 (2005) 1665–1667.
[43] Private communication with M. Wakeda, and S. Ogata.